



# Effect of Annealing Time on the Microstructure and Mechanical Properties of Lightweight Medium Manganese Steel

Z. L. Wu, C. N. Jing<sup>(✉)</sup>, Z. T. Li, Y. Feng, T. Lin, and J. R. Zhao

College of Materials Science and Engineering, Shandong Jianzhu University, Jinan 250101, China  
jcn@sdjzu.edu.cn

**Abstract.** The purpose of this paper is to look at how annealing time affects the microstructure and mechanical characteristics of lightweight medium manganese steel. OM, XRD, SEM, and other characterization methods were used to examine and test the microstructure. The findings revealed that the test steels' microstructures were all composed of martensite,  $\alpha$ -ferrite,  $\delta$ -ferrite, and retained austenite. The retained austenite content of the test steel appears to increase after a certain time of annealing treatment. The TRIP effect created by stretching increases the mechanical properties of the test steel.

**Keywords:** Medium manganese steel · Microstructure · Work-hardening · Strength and plasticity

## 1 Introduction

In recent years, the automotive industry has shifted toward reduced weight and more safety. As energy consumption and environmental issues grow more significant, increased demands are put on steel used in vehicles. Improving the strength of automotive steels and reducing material density are important ways to accomplish lightweighting [1–3]. The present third generation of automobile steel is based on combining the inclusion of lightweight materials for “lightness” with strengthened plasticization for “thinness.” Medium manganese steel, the most promising new generation of advanced high-strength automotive steel, has become a hot spot for domestic and international research because of its combined high strength and high plasticity, which can well meet the requirements of automobile light weight and safety [4]. As a series of Mn steels, the Fe-Mn-Al-C system is the focus of the current study by adding lightweight Al elements and austenite-stabilized Mn elements to the steel to enlarge the austenite phase zone and therefore achieve a significant quantity of austenite with definite stability at room temperature [5]. Currently, the critical annealing (IA) process, i.e., austenite reduction phase transformation of martensite between the ferrite and austenite two-phase zones, is used to manufacture medium manganese steels, including ferrite and sub-stable austenite grains [6, 7]. The TRIP effect of sub-stable austenite improves the ductility and tensile

strength of medium manganese steels [8, 9]. Shi [10] and Mishra [11] studied the (0.2–0.4 wt.%) C-(5–7 wt.%) Mn and 0.18C-5Mn (wt.%)*-based cold-rolled medium manganese steels by adjusting the annealing temperature in the two-phase zone to achieve the product of strength and elongation 40 GPa·%, respectively. De Cooman [12] demonstrated excellent yield strength and ultra-high tensile strength for Fe-0.29C-6.1Mn-2.2Al-1.5Si-0.23V (wt.%) steel by combining IA with quenching and partitioning (Q&P) treatment of critical austenite, resulting in a higher overall performance of the test steel.*

As can be seen, the medium manganese steel may be manufactured to have an excellent balance of strength and plasticity by adjusting the process parameters throughout the heat treatment process. Based on the critical annealing and Q&P processes, this paper investigates the effects of different annealing times on the microstructure and mechanical properties of lightweight medium manganese steel, with the hope of serving as a reference for adjusting annealing process parameters in the actual production process.

## 2 Experiment Section

Cold-rolled low carbon silicon manganese steel with a thickness of 1.5 mm was employed in this study, and its chemical composition and percentage content were reported in Table 1.

JMatPro simulation software was used to measure the temperature of the heat treatment process, and the temperatures determined for  $A_{C3}$  and  $A_{C1}$  were 1227 °C and 728 °C, respectively. The requisite tensile specimens were manufactured using an ASTM E8 wire-cutting process.

First, the test steel was kept in the two-phase zone at 750 °C for 0, 15, and 30 min. After that, it was quickly placed in a 25 °C water bath and held for the 90 s. Finally, the test steel was cooled to room temperature using water. In this research, the specimens

**Table 1.** Chemical composition of test steel (wt.%).

Composition	C	Mn	Al	Si	Cu	Mo	Cr	Nb	B	Fe
Content	0.09	7.23	4.42	1.99	0.5	0.2	0.33	0.11	0.001	bal

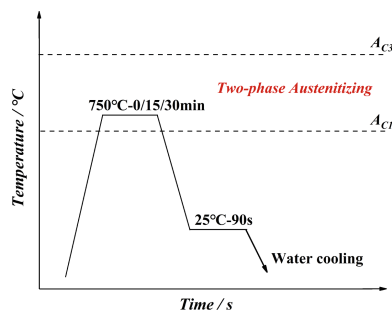


**Fig. 1.** Heat treatment process.

with varying holding times in the two-phase area were designated as A0, A15, and A30 for ease of presentation. The heat treatment process is shown in Fig. 1.

The specimens were ground and polished before being etched with 4% ethanol nitrate. For microstructure testing, the samples were examined by OM electron microscopy, an x-ray diffractometer (XRD, RIKEN Smart Lab), and field emission scanning electron microscopy (FE-SEM, SUPRATM 55). Using the following equation [13], the austenite peaks  $(200)\gamma$ ,  $(220)\gamma$ ,  $(311)\gamma$ , and ferrite peaks  $(200)\alpha$ ,  $(211)\alpha$  of the XRD patterns were utilized to compute the content of retained austenite and the quantity of carbon contained in the retained austenite.

$$V_i = \frac{1.4I_\gamma}{I_\alpha + 1.4I_\gamma} \quad (1)$$

$$a_{\gamma/\alpha} = \frac{\lambda\sqrt{h^2 + k^2 + l^2}}{2 \sin \theta} \quad (2)$$

$$w(C_\gamma) = \frac{a_\gamma - 3.547}{0.046} \quad (3)$$

Where:  $V_i$  - volume fraction of retained austenite;  $I_\alpha$  - cumulative intensity of ferrite peaks;  $I_\gamma$  - cumulative intensity of austenite peaks.  $C_\gamma$  is the mass fraction (%) of carbon in the retained austenite;  $a_\gamma$  is the lattice constant on the surface of the retained austenite crystal;  $C_\alpha$  is the mass fraction (%) of carbon in the martensite.  $a_\alpha$  is the lattice constant on the surface of the martensite crystal.

### 3 Results and Discussion

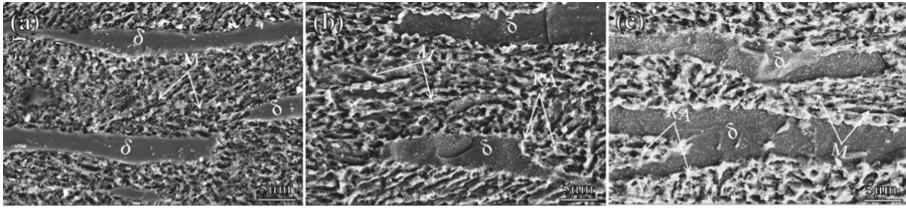
#### 3.1 Microstructure

OM optical electron microscopy was used to observe the specimens, as shown in Fig. 2. The black section was martensite, whereas the white section was austenite/ferrite. The microstructure of the test steel can be observed to have a clear rolling direction. Because cold rolling has a high depression rate, the original microstructure of the test steel grain was broken a lot, and this was accompanied by the generation of the grain penetration phenomenon.

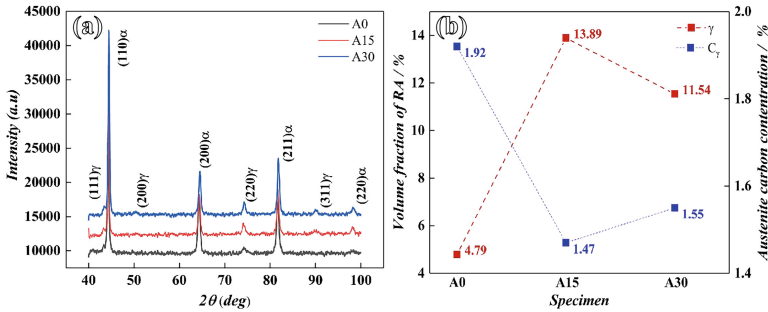
The specimens were analyzed by SEM observation, as shown in Fig. 3. This enables the identification of a multiphase microstructure of the test steel consisting primarily of  $\alpha$ -ferrite( $\alpha$ ),  $\delta$ -ferrite( $\delta$ ), retained austenite (RA), and martensite (M).



Fig. 2. OM microstructure observation: (a) A0 specimen, (b) A15 specimen, (c) A30 specimen.



**Fig. 3.** SEM microstructure observation: (a) A0 specimen, (b) A15 specimen, (c) A30 specimen.



**Fig. 4.** (a) XRD diffraction analysis, (b) retained austenite content and carbon content in retained austenite.

The XRD patterns, retained austenite content, and retained austenite carbon content variation curves of the test steels are shown in Fig. 4. There was no significant intensity of the  $\{200\}\gamma$  and  $\{311\}\gamma$  diffraction peaks in the A0 specimen. Meanwhile, the  $\{220\}\gamma$  diffraction peak had a lower intensity than the A15 and A30 specimens. It can be shown that a certain duration of intercritical annealing of the test steel may enhance the amount of retained austenite in the test steel.

### 3.2 Mechanical Properties

The specimens were stretched at room temperature, and their stress-strain and work-hardening curves are shown in Fig. 5. It was discovered that the work-hardening curves of A15 and A30 specimens occur in 4 stages: rapid rising (S1 stage), fast falling (S2 stage), slow falling (S3 stage), and fast falling (S4 stage). Work-hardening curves for A0 specimens, on the other hand, were only ever-present for the S1 and S2 stages. As a consequence, the A0 specimen has low plasticity. It can be shown that A15 and A30 have virtually similar work-hardening curves, resulting in approximately the same elongation.

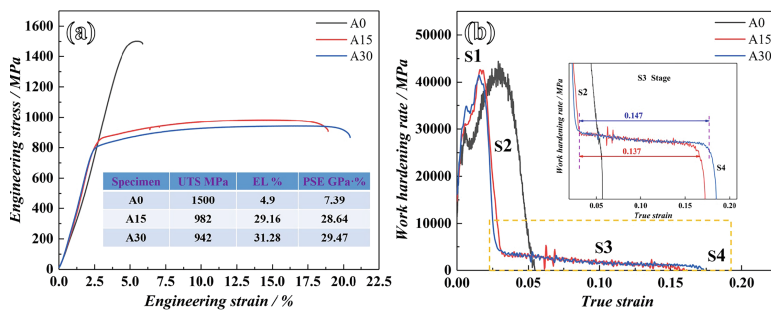


Fig. 5. (a) Stress-strain curve, (b) Work-hardening curve.

## 4 Conclusions

- (1) The microstructure grain of medium manganese steel steadily increases, and the tensile strength gradually declines after a certain time of annealing treatment.
- (2) Medium manganese steel, after a certain period of annealing treatment, can increase the content of retained austenite in the microstructure, thereby improving the overall mechanical properties of the test steel.
- (3) When the microstructure and mechanical properties of A15 and A30 were compared, it is clear that the shorter annealing process can also optimize the performance of the test steel while saving energy in the manufacturing process, providing some theoretical guidance for the adjustment of the actual heat treatment process parameters for automotive steels.

**Acknowledgments.** This work was supported by the National Natural Science Foundation of China (Grant number No. 51871136).

## References

1. Y. K. Lee and J. Han, Current opinion in medium manganese steel, *Mater. Sci Tech-Lond.* **31**, 843 (2015).
2. J. H. Chung, J. B. Jeon and Y. W. Chang, Work-hardening and ductility enhancement mechanism of cold rolled multiphase TRIP steels, *Met. Mater. Int.* **16**, 533 (2010).
3. T. L. Wang, Y. Lu, F. Z. Ren, S. Z. Wei and B. H. Tian, Research progress of ultra-high strength low alloy steels, *Heat Treatment of Metals* **40**, 13 (2015).
4. S. B. Bai, W. Q. Wei, W. T. Xiao, W. Liang and D. Z. Li, Research progress and future Research prospect of medium Mn steels, *Hot Working Technol.* **51**, 1 (2022).
5. R. B. Song, W. F. Huo, N. P. Zhou, J. J. Li, Z. R. Zhang and Y. J. Wang, Research progress and prospect of Fe–Mn–Al–C medium Mn steels, *Chinese J. Eng.* **42**, 814 (2020).
6. C. W. Shao, W. J. Hui, Y. J. Zhang, X. L. Zhao and Y. Q. Weng, Microstructure and mechanical properties of hot-rolled medium-Mn steel containing 3% aluminum, *Mater. Sci Eng. A.* **682**, 45 (2017).

7. Z. H. Cai, H. Ding, R. D. K. Misra and Z. Y. Ying, Austenite stability and deformation behavior in a cold-rolled transformation-induced plasticity steel with medium manganese content, *Acta Mater.* **84**, 229 (2015).
8. K. I. Sugimoto, B. Z. Yu, Y. I. Mukai and S. S. Ikeda, Microstructure and formability of aluminum bearing TRIP-Aided steels with annealed martensite matrix, *ISIJ Int.* **45**, 1194 (2005).
9. C. F. Meng, Y. D. Wang, Y. H. Wei, B. Q. Shi, T. X. Cui and Y. T. Wang, Strengthening mechanisms for Ti- and Nb-Ti-micro-alloyed high-strength steels, *J. Iron Steel Res. Int.* **23**, 350 (2016).
10. J. Shi, X. J. Sun, M. Q. Wang, W. J. Hui, H. Dong and W. Q. Cao, Enhanced work-hardening behavior and mechanical properties in ultrafine-grained steels with large-fractioned metastable austenite, *Scripta Mater.* **63**, 815 (2010).
11. G. Mishra, A. K. Chandan and S. Kundu, Hot rolled and cold rolled medium manganese steel: Mechanical properties and microstructure, *Mater. Sci. Eng. A* **701**, 319 (2017).
12. S. Lee and B. C. De Cooman, Tensile behavior of intercritically annealed 10 pct Mn multi-phase steel, *Metall. Mater. Trans A.* **45**, 709 (2014).
13. Z. Li and D. Wu, Effects of hot deformation and subsequent austempering on the mechanical properties of Si-Mn TRIP steels, *ISIJ Int.* **46**, 121 (2006).

**Open Access** This chapter is licensed under the terms of the Creative Commons Attribution-NonCommercial 4.0 International License (<http://creativecommons.org/licenses/by-nc/4.0/>), which permits any noncommercial use, sharing, adaptation, distribution and reproduction in any medium or format, as long as you give appropriate credit to the original author(s) and the source, provide a link to the Creative Commons license and indicate if changes were made.

The images or other third party material in this chapter are included in the chapter's Creative Commons license, unless indicated otherwise in a credit line to the material. If material is not included in the chapter's Creative Commons license and your intended use is not permitted by statutory regulation or exceeds the permitted use, you will need to obtain permission directly from the copyright holder.

